THE JOURNAL OF BIOLOGICAL CHEMISTRY
Vol. 276, No. 7, Issue of February 16, pp. 5353–5359, 2001

Printed in U.S.A.

Hypercontractile Properties of Cardiac Muscle Fibers in a Knock-in Mouse Model of Cardiac Myosin-binding Protein-C*

Received for publication, September 22, 2000, and in revised form, November 1, 2000
Published, JBC Papers in Press, November 28, 2000, DOI 10.1074/jbc.M008691200

Christian C. Witt‡§, Brenda Gerull‡, Michael J. Davies¶, Thomas Centner‖, Wolfgang A. Linke‡‡, and Ludwig Thierfelder‡**

*From the ‡Max-Delbrück-Center of Molecular Medicine, D-13122 Berlin, Germany, the §Institut für Anästhesiologie und Operative Intensivmedizin, Universitätsklinikum D-68167 Mannheim, Germany, the ¶St. George's Hospital Medical School, British Heart Foundation Cardiovascular Pathology Unit, London, SW170RE United Kingdom, the ‖European Molecular Biology Laboratory, D-69012 Heidelberg, and the **Institute of Physiology and Pathophysiology, University of Heidelberg, D-69120 Germany*

Myosin-binding protein-C (MyBP-C) is a component of all striated-muscle sarcomeres, with a well established structural role and a possible function for force regulation. Multiple mutations within the gene for cardiac MyBP-C, one of three known isoforms, have been linked to familial hypertrophic cardiomyopathy. Here we generated a knock-in mouse model that carries N-terminal-shortened cardiac MyBP-C. The mutant protein was designed to have a similar size as the skeletal MyBP-C isoforms, whereas known myosin and titin binding sites as well as the phosphorylatable MyBP-C motif were not altered. We have shown that mutant cardiac MyBP-C is readily incorporated into the sarcomeres of both heterozygous and homozygous animals and can still be phosphorylated by cAMP-dependent protein kinase. Although histological characterization of wild-type and mutant hearts did not reveal obvious differences in phenotype, left ventricular fibers from homozygous mutant mice exhibited an increased Ca^{2+} sensitivity of force development, particularly at lower Ca^{2+} concentrations, whereas maximal active force levels remained unchanged. The results allow us to propose a model of how cMyBP-C may affect myosin-head mobility and to rationalize why N-terminal mutations of the protein in some cases of familial hypertrophic cardiomyopathy could lead to a hypercontractile state.

Myosin-binding protein-C (MyBP-C)[1] (1, 2) is a myofibrillar protein that contributes to the structural integrity of the sarcomere and possibly is involved in the regulation of contraction (3). Three different isoforms of MyBP-C have been identified: skeletal (sMyBP-C), fast and slow, and a cardiac-specific variant (cMyBP-C, see Fig. 1*A*), each of these being coded for by a distinct gene (4, 5). All isoforms interact at the C terminus with the rod portion of myosin (*e.g.* Ref. 6), as well as with titin (*e.g.* Ref. 7), and thus help maintain an ordered thick-filament structure (reviewed in Ref. 3). MyBP-Cs are modular polypeptides that belong to the intracellular immunoglobulin (Ig) superfamily. Whereas the skeletal variants consist of 10 globular domains of the Ig-like or fibronectin-type-III-like fold (4), cMyBP-C contains an additional N-terminal Ig module termed C0 (5). Between the Ig domains C1 and C2, MyBP-Cs also contain a stretch of about 100 residues, the MyBP-C motif (see Fig. 1*A*), which in cardiac muscle can be phosphorylated at three sites by cAMP-dependent protein kinase (8). The MyBP-C motif was shown to bind to the S-2 segment of myosin, close to the lever arm domain of the myosin head (9). Interestingly, this interaction is dynamically regulated by phosphorylation/dephosphorylation of the MyBP-C motif (10). Moreover, the controlled interaction with the myosin hinge region appears to affect the contractile behavior of muscle fibers (11) and thus, could represent a potential regulatory mechanism of contractility (12). These insights notwithstanding, direct evidence for a role of cMyBP-C in force regulation has been difficult to obtain.

Uncovering the functions of cMyBP-C is interesting from a clinical point of view as the protein is involved in the pathophysiology of familial hypertrophic cardiomyopathy (FHC, Refs. 13, 14). This inherited disease occurs in autosomal-dominant fashion and affects ~0.2% of the general population. FHC is known to be a disease of the sarcomere; mutations in at least eight different sarcomeric protein genes have been identified as yet (14, 15). Mutations in *cMYBPC* account for ~15–20% of genetically defined FHC cases, but the cMyBP-C-linked types of FHC present as relatively benign phenotypes with mild hypertrophy at mid-life (16, 17). Most cMyBP-C lesions show C-terminal truncated polypeptides lacking either the myosin or myosin and titin binding sites, but some lesions are also caused by missense mutations occurring in more N-terminal regions of the protein (16). Genetical engineering approaches have been used to generate transgenic mice lacking variable numbers of C-terminal domains of cMyBP-C (18–20). These model systems have demonstrated the importance of the C terminus of cMyBP-C for a regular sarcomeric structure and normal contractility of the heart.

In the present study we used knock-out/knock-in technology to generate mice (hereafter termed knock-in mice) with N-terminal deletion of a region of cMyBP-C comprising one Ig domain and a linker sequence next to the MyBP-C motif. The shortened cMyBP-C (see Fig. 1*A*) thus has a domain structure similar to that of sMyBP-C. Notably, within the region affected by the knock-in, a missense mutation has been described for a family of FHC patients exhibiting a distinct phenotype (16). We show that the cMyBP-C deletion variant is expressed in both

* This work was supported by the Max-Delbrück Center for Molecular Medicine (twinning grant), the Deutsche Forschungsgemeinschaft (Li690/5-1, La668/5-1), and the Medical Faculty of the University of Heidelberg (Forschungsförderungsprogramm). The costs of publication of this article were defrayed in part by the payment of page charges. This article must therefore be hereby marked "*advertisement*" in accordance with 18 U.S.C. Section 1734 solely to indicate this fact.

‡‡ To whom correspondence should be addressed: Inst. of Physiology and Pathophysiology, University of Heidelberg, Im Neuenheimer Feld 326, D-69120, Heidelberg, Germany. Tel.: 49-6221-544130 or 544135; Fax: 49-6221-544049; E-mail: wolfgang.linke@urz.uni-heidelberg.de/

[1] The abbreviations used are: MyBP-C, myosin-binding protein-C; PCR, polymerase chain reaction; RT-PCR, reverse transcriptase PCR; TK, thymidine kinase; ES, embryonic stem cell; FHC, familial hypertrophic cardiomyopathy; kb, kilobases.

homozygous and heterozygous mice at the protein level and is readily incorporated into the sarcomere. Animals carrying the deletion are viable, show no significant ultrastructural changes of the heart, and appear to have a normal life span. Mutated cMyBP-C could still be phosphorylated by cAMP-dependent protein kinase, but skinned muscle fibers from homozygous mutant hearts revealed a leftward shift in the force-pCa curve and a decreased slope of that curve. The increased Ca^{2+} sensitivity may result from decreased steric hindrance of myosin-head mobility caused by the expression of the shorter cMyBP-C. We discuss the possibility that the additional N-terminal Ig domain present in cardiac *versus* skeletal MyBP-C could be included by nature to aid force regulation at the cross-bridge level in the heart. Our findings also provide a starting point to explain the development of hypertrophied cardiac tissue in FHC cases with N-terminal mutations of cMyBP-C.

EXPERIMENTAL PROCEDURES

Gene Targeting—A P1 clone containing the murine cardiac MYBP-C sequence was obtained from a mouse 129 P1 genomic library (Genome Systems, St. Louis, MO). A 9.1-kb *Eco*RI fragment from the P1 clone was isolated and subcloned and found to contain the 5′-end of the gene from exon 1–20 (Fig. 1*B*). A 1.7-kb *Stu*I/*Eco*RV fragment (including exon 2) located upstream of exon 3 and a 5.3-kb NsiI/*Eco*RI fragment (including exon 7–20) located downstream of exon 6 were used as the 5′ and 3′ homology units.

The targeting vector was constructed by standard recombinant techniques. A genomic fragment of the *MYBP-C* gene (1.3 kb) including exons 3–6 was deleted and replaced by a neomycin resistance gene (Fig. 1*B*). The vector contained a herpes simplex thymidine kinase cassette for negative selection of single recombinant embryonic stem (ES) cell clones. Also, the vector included a unique *Cla*I restriction site for linearization of the plasmid. Homologous recombination between targeting vector and cognate cMyBP-C locus deleted exons 3–6. Colony selection and target clone identification were done as described elsewhere (21). Targeting vector (20 μg) was introduced into 1.2×10^7 ES cells by electroporation. Genomic DNA was prepared as described (22). Correct targeting of G418-resistant clones was analyzed by Southern blotting.

Clones were subsequently tested by long PCR assay (Combi Pol/InViTek, Berlin-Buch). To check for the occurrence of new recognition sites on the amplificates, Southern blotting was employed. Correctly targeted clones were microinjected into C57/BL 6 blastocysts, which were implanted into pseudo-pregnant CB6 mice bred to produce heterozygous or homozygous mutant animals.

MyBP-C mRNA was assessed by nucleotide sequence analysis of RT-PCR-amplified DNA fragments according to standard protocols. The following primer pairs were used: CF 198, GGCTGAGACGGAGCGGTCAGGCG; CR 558, GTCATCAGGGGCTCCCTGATGCTCTGCAGC; CF 198, GGCTGAGACGGAGCGGTCAGGCG; CR1134, CGAAGGTCTGTGACTCCGTGCTGG; CF3923, CAGGATGGCTCCCCAGAGATGGCT; and CR4195, GCTCCTACACAATGAGCCAGCCAG. Northern blotting of cardiac/skeletal-muscle RNA was performed as described previously (23).

Morphology and Microscopy—Excised hearts were rinsed in 4% paraformaldehyde and weighed, and cardiac tissue was examined for pathological alterations (24). Examined parameters included heart weight, left ventricular wall thickness and cavity size, and myocyte nuclear size (measured by outlining the nucleus in 150 cardiac cells cut in their long axis).

Indirect Immunofluorescence Microscopy—Bundles of myofibrils prepared from left ventricle essentially as described (25) were examined under a Zeiss Axiovert 135 microscope. MyBP-C was visualized by using antibodies against the MyBP-C motif (25).

Cardiac Fiber Mechanics—Freshly excised mouse hearts were perfused retrogradely through the aorta with 4 °C rigor buffer (mM: NaCl, 132; KCl, 5; $MgCl_2$, 1; glucose, 7; *N*-tris(hydroxymethyl)methyl-2-aminoethanesulfonic acid, 10; pH 7.0; EGTA, 5; leupeptin, 0.1; and 2,3-butanedione monoxime (BDM, Ref. 20) for 2 min. Papillary muscles or trabeculae from left ventricle were dissected, tied to thin glass rods, and skinned overnight in ice-cold relaxing solution (mM: imidazole, 20; pH 6.8; ATP, 7.5; $MgCl_2$, 10; NaN_3, 1; EGTA, 4; leupeptin, 0.1; BDM, 20; total ionic strength, 130) containing 0.25–0.5% Triton X-100 (26). A relatively low buffer pH used in skinned fiber mechanical studies was reported to be beneficial for the functional preservation of the regulatory system (27). After washes with fresh relaxing buffer, fiber bundles 150–200 μm thin and 3–4 mm long were mounted isometrically between a position-controlled rigid post and a force transducer (AME AE 801, Horten Electronics, Norway) with nitroacetate glue (26). Sarcomere length was adjusted to 2.2 μm by laser diffractometry. After removal of BDM and addition of an ATP-regenerating system (creatine phosphate, 10 mM; creatine kinase, 150 units/ml) to the solution, fibers were activated by transfer from relaxing to activating buffer, in which EGTA was substituted by Ca^{2+}-EGTA. The desired Ca^{2+} concentration was calculated as described (26). Experiments were carried out at room temperature.

The normalized force-pCa relationships, in which force was expressed relative to the maximum force usually developed at pCa 4.34, were fitted to the Hill equation,

$$f/f_{max} = [Ca^{2+}]^{HC}/(K_c + [Ca^{2+}]^{HC}) \quad \text{(Eq. 1)}$$

where *HC* (the Hill coefficient, a measure of cooperativity) and K_c are constants.

Gel Electrophoresis and ^{32}P Autoradiography—Fiber bundles prepared as described above were washed with relaxing solution (ATP, 4 mM). Specimens were incubated with the catalytic subunit of protein kinase A (Sigma, 500 units/ml relaxing buffer) in the presence of [γ-^{32}P]ATP (specific activity, 250 μCi/μM) for 45 min at room temperature (26, 28). Proteins were then denatured, dissolved, and electrophoresed on 8% SDS-polyacrylamide gels. Major myofibrillar proteins were identified by Coomassie staining. ^{32}P incorporation was visualized by autoradiography, using a 4–12-h exposure time with standard Kodak x-ray film (28, 29).

RESULTS

Generation of Mutant cMyBP-C Mice—To target the *MYBP-C* gene, a 9.1-kb fragment of the murine cardiac MYBP-C locus encompassing exons 1–20 was isolated and subcloned (Fig. 1*B*). The targeting construct was designed to selectively remove exons 3–6 (1.3 kb) thus producing a deletion of the Ig domain C1 and the linker region between domains C0 and C1 of cMyBP-C (Fig. 1*A*). Fig. 1*B* illustrates the cardiac *MYBP-C* locus and the gene-targeting construct containing a neomycin (*NEO*) resistance gene and a herpes simplex thymidine kinase cassette (TK) to allow for negative selection. Fig. 1*B* (*bottom*) depicts the cMyBP-C deletion mutant obtained after electroporation of the linearized plasmid into ES cells and homologous recombination between the targeting vector and the cognate *MYBP-C* locus.

Ninety-six G418-resistant ES cell clones were analyzed, and genomic Southern blotting of DNA from ES cell clones was performed to detect the targeting event. Correct targeting was found in 6 clones. As shown in Fig. 2*A*, a band corresponding to a 9.1-kb fragment was detected as the wild-type allele, and a band corresponding to a 2.7-kb fragment as the targeted allele. Correctly targeted clones were used for blastocyst-mediated transgenesis and production of chimeric animals. Appropriate breeding produced mice either homozygous or heterozygous for the cMyBP-C deletion. These mice were fertile, produced normal litter sizes, and survived for >1 year. We also tested the correctly targeted clones in a long PCR assay. Primers were designed such that a 2.2-kb fragment was produced specific for the wild-type allele and a 1.9-kb fragment specific for the targeted allele (data not shown). Additionally, a PCR was done with a 4.8-kb product (Fig. 1*B*, *top*). The analysis showed that the restriction enzyme *Eco*RI cut the amplificate only of the targeted allele into a 2.8 and a 2.0 kb fragment (Fig. 2*B*), indicating the introduction of a new recognition site.

cMyBP-C Expression in Mutant Mice—To determine the expression of cMyBP-C transcripts in mutant mice, we performed RT-PCR analysis with various primer pairs from different regions of heart cDNA (Fig. 2*C*). With a primer pair encompassing domains C0 to C1, a signal was obtained only for cDNA from wild-type or heterozygous mice, whereas in homozygous

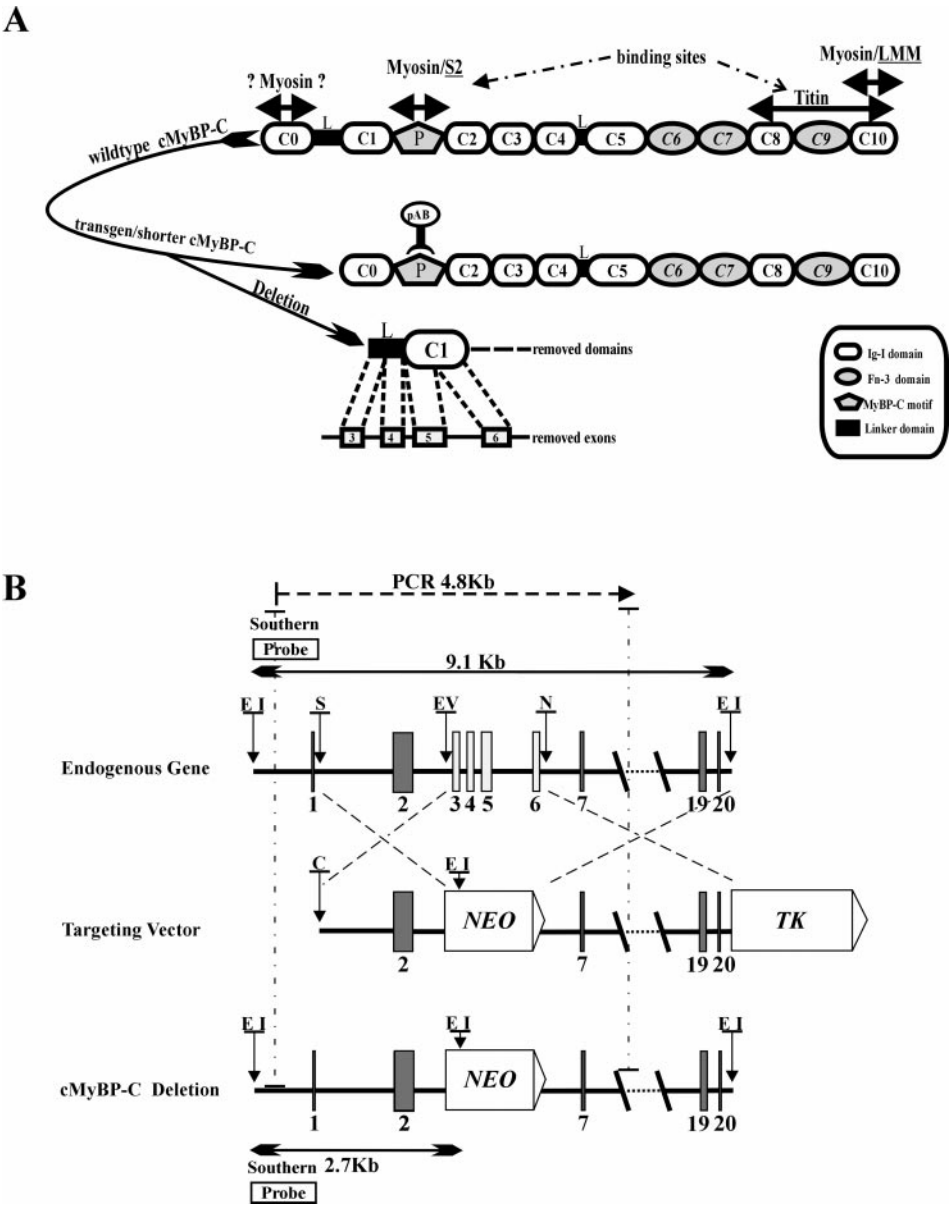

FIG. 1. **Structure of cMyBP-C and gene-targeting strategy.** *A,* domain architecture of normal cMyBP-C and the N-terminal deletion mutant. The deletion results in loss of the linker sequence between modules C0 and C1 and of the C1 domain. Shown are the established binding sites of MyBP-C to the rod (*LMM*) portion of myosin, to titin, and to the myosin neck region (*S2*), as well as the proposed C0-domain binding site to the myosin (head). The recognition site of a polyclonal antibody against the MyBP-C motif (*pAB*) used in this study is also indicated. *B,* schematic of the genomic structure of wild-type MyBP-C and MyBP-C(Neo) alleles. Exons 1–7 and 19–20 are depicted for each allele. The mutation removes exons 3–6 (1.3 kb), all other exons are identical. The *bottom part* indicates the MyBP-C deletion mutant obtained after electroporation of the plasmid into ES cells. For further details on the targeting strategy, see text.

mutant animals, RNA encoding the C1 domain plus N-terminal adjacent linker was not expressed (Fig. 2*C*, *panel a*). This observation is consistent with the results of Northern blot analyses (Fig. 2*D*). No signal was detected when total RNA, isolated from homozygous hearts, was hybridized with a C1+linker probe. By contrast, a signal was detectable in heterozygous hearts. In comparison, when skeletal-muscle RNA was used, no signal was present (Fig. 2*D*). Hybridization with a probe of the MyBP-C motif revealed a normal signal for heart RNA in all types of animals, but none for skeletal-muscle RNA. Controls with a GAPDH probe showed a signal in all lanes.

By RT-PCR, using primer pairs encompassing the C0 domain and the MyBP-C motif, we detected the expected deletion of 474 base pairs (Fig. 2*C*, *panel b*). Cloning and sequencing of the products highlighted by the *asterisks* (Fig. 2*C*) revealed that the upper band corresponds to the wild-type DNA sequence, whereas the lower band product has the same flanking sequence but contains the predicted deletion. We note that in competitive PCR, a shorter product tends to show a larger signal than a longer product, as seen in Fig. 2*C*, *panel b*. This figure, as well as the RT-PCR at the 3′-untranslated region (Fig. 2*C*, *panel c*), demonstrate that the transgenic RNA is stable and well expressed; no degradation or lowered expression was detectable. Thus, regulation at the transcription level seems unlikely.

Both homozygous and heterozygous mice were found to express the deletion mutant also at the protein level. Western blot analyses with muscle protein obtained from all types of animals revealed a distinct band stained by a polyclonal antibody against the MyBP-C motif (Fig. 3*A*). Moreover, cardiac myofibrils labeled with fluorophore-marked α-MyBP-C antibodies exhibited the expected staining pattern in the sarcomeric A-band; no obvious difference in staining intensity or regularity of labeling was found between wild-type and homozygous mutant animals (Fig. 3*B*). Thus, mutant mice stably expressed the shortened cMyBP-C protein.

Histological Characterization—Hearts from several months (up to ~1 year) old animals ($n = 7$, for each animal type) were examined for histological and morphological abnormalities (Table I). None of the parameters investigated differed between animal types in a statistically significant manner, although one homozygous mutant heart revealed an abnormal phenotype with strongly increased values for all four parameters. In general, however, no evidence was found for cardiac hypertrophy,

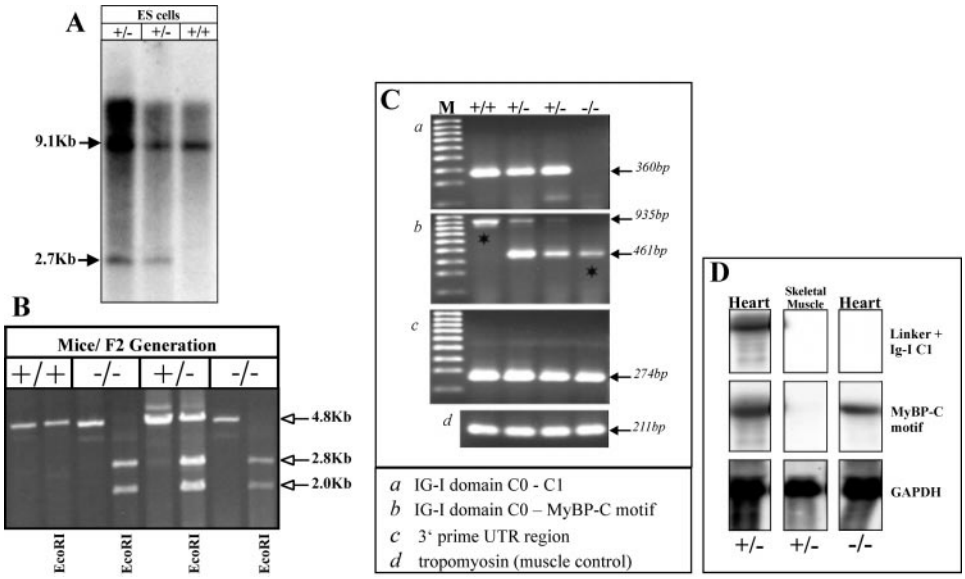

FIG. 2. **Expression of mutant cMyBP-C.** *A,* Southern blot analysis of DNA to show correct targeting in ES cell clones; the 9.1-kb band is specific to the wild-type allele, the 2.7-kb band to the targeted allele. *B,* PCR-based genotypic analysis of wild-type (+/+), heterozygous (+/−) and homozygous (−/−) mutant mice. The 4.8-kb amplificate covers the length indicated in Fig. 1. Only the targeted allele is cut into two subfragments by the restriction enzyme *Eco*RI revealing the introduction of a new recognition site. *C*, RT-PCR analysis of cDNA to show expression of cMyBP-C transcripts in wild-type and mutant mice. Various primer pairs encompassing different regions of cDNA of cMyBP-C were used, as indicated for each *panel*; *panel d* is a control with tropomyosin. The *asterisks* in *panel b* highlight the products subsequently cloned and sequenced. *D,* Northern blot analysis of RNA from heart and (for comparison) skeletal muscle. The results confirm the lack of expression of the C0-C1 linker sequence and of the entire C1 domain of cMyBP-C in homozygous mutant mice. Controls were done with GAPDH probes.

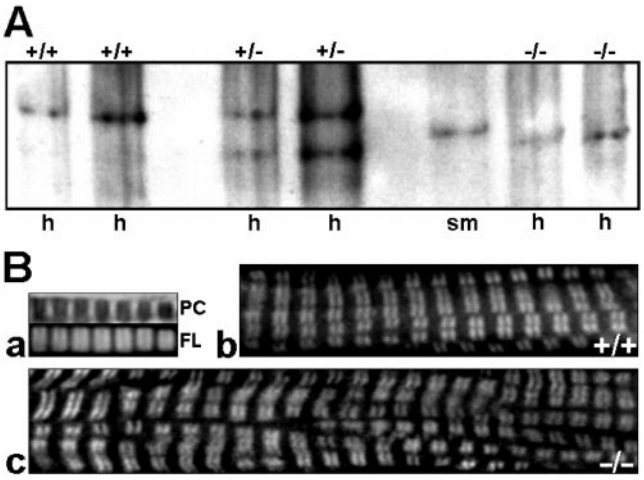

FIG. 3. **MyBP-C expression at the protein level.** *A,* Western blot of wild-type (+/+), heterozygous (+/−), and homozygous (−/−) mutant hearts (*h*), using a polyclonal antibody against the MyBP-C motif. The antibody cross-reacts with skeletal-muscle (*sm*) MyBP-C. *B*, immunofluorescence microscopy on cardiac myofibrils, using the α-MyBP-C antibody, which stained the expected two epitopes in the sarcomeric A-band region (*panel a*: *PC,* phase-contrast image; *FL,* fluorescence image). The staining pattern was the same in myofibrils from wild-type (*panel b*) and homozygous mutant (*panel c*) hearts.

myocyte loss or inflammation. Thus, the histological appearance of heterozygous or homozygous mutant hearts appeared to be normal.

Fibers from Homozygous Mutant Hearts Show Increased Ca^{2+} Sensitivity of Force Generation—Left ventricular muscle strips obtained from wild-type and mutant, litter-matched, animals were probed for their contractile properties by measuring the active force of skinned fiber bundles as a function of the Ca^{2+} concentration. Because the Ca^{2+} sensitivity varies with sarcomere length, laser diffractometry was used to set this length to 2.2 μm in all experiments. A typical example demonstrating the force rise with increasing [Ca^{2+}] (*i.e.* decreasing pCa) is shown in Fig. 4, *inset*. Fibers from 5 wild-type, 2

TABLE I
Summary of results of morphological measurements

Data are presented as mean ± S.D. $n = 7$ for wildtype (WT), heterozygous mutant (+/−), and homozygous mutant (−/−) hearts.

	Heart weight	LV wall thickness	LV cavity	Myocyte nuclear size
	g	*mm*	*mm*	μm^2
WT	0.255 ± 0.049	1.09 ± 0.30	4.09 ± 0.44	48.71 ± 15.18
+/−	0.289 ± 0.048	1.17 ± 0.21	4.49 ± 0.79	44.00 ± 14.14
−/−	0.274 ± 0.049	1.16 ± 0.35	4.31 ± 0.42	52.57 ± 13.88

cMyBP-$C^{(+/-)}$, and 6 cMyBP-$C^{(-/-)}$ mice were included in the analysis, and 5–7 fiber bundles per animal were investigated. A summary of results is presented in Fig. 4. Fibers from wild-type and heterozygous mutant mice exhibited a similar Ca^{2+} sensitivity of force development, with pCa_{50} values (pCa at half-maximum force) of 5.19 ± 0.01 S.E. and 5.18 ± 0.01 S.E. and Hill coefficients of 3.14 ± 0.06 S.E. and 3.00 ± 0.05 S.E., respectively. In contrast, homozygous mutant mice showed a statistically significant increase in Ca^{2+} sensitivity (pCa_{50} = 5.26 ± 0.02) and a decreased slope of the force-pCa curve (Hill coefficient, 2.32 ± 0.20). Thus, the Ca^{2+} sensitivity of force generation was particularly increased at low to modest physiological [Ca^{2+}], the concentrations relevant to normally working cardiac muscle. No statistically significant difference was found between animal types with regard to the (absolute) maximum active force levels ($p > 0.05$ in unpaired Student's *t* test). This indicates that the increase in relative force observed in the cMyBP-$C^{(-/-)}$ fibers mainly at lower [Ca^{2+}] is not offset by a change in the maximum force level.

The N-terminal Deletion Mutant Is Still Phosphorylated by cAMP-dependent Protein Kinase—To find out whether the altered Ca^{2+} sensitivity could be related to an altered response of the mutant cMyBP-C to activation by cAMP-dependent protein kinase (because the deletion is close to the MyBP-C motif), we tested the ability of the protein to be phosphorylated by this kinase (see Refs. 28, 30, 31). As shown in Fig. 5, autoradiography of SDS-polyacrylamide gels of left ventricular tissue incubated with the catalytic subunit of cAMK in the presence of

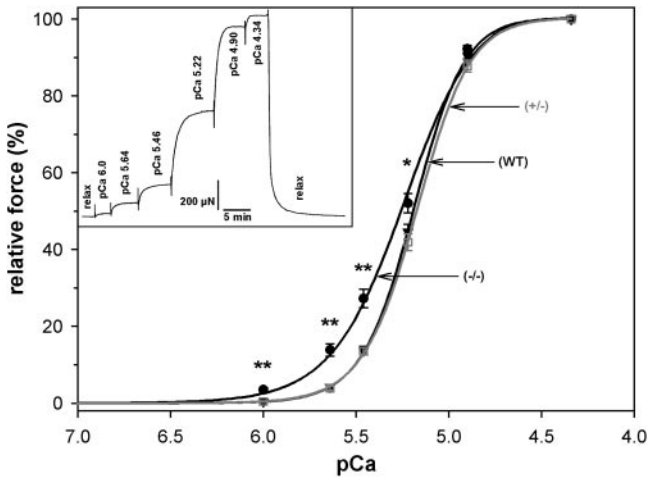

FIG. 4. **Cardiac fiber mechanics.** Skinned fiber bundles were activated at a sarcomere length of 2.2 μm at a series of different Ca^{2+} concentrations, from pCa 6.0 to pCa 4.34, and forces were recorded (*inset*). Force was expressed relative to the maximal force level reached at optimal [Ca^{2+}]. A summary of results shows that wild-type ($n = 32$) and heterozygous mutant fibers ($n = 10$) exhibited a similar Ca^{2+} sensitivity of force development. In contrast, Ca^{2+} sensitivity of homozygous mutant fibers ($n = 38$) was significantly increased at modest to high pCa. The pCa_{50} value was shifted leftward by 0.07 pCa units; the slope of the curve was decreased. Statistically significant differences to wild-type specimens were confirmed by unpaired Student's *t* test (*, $p < 0.05$; **, $p < 0.001$). Values are mean ± S.E.

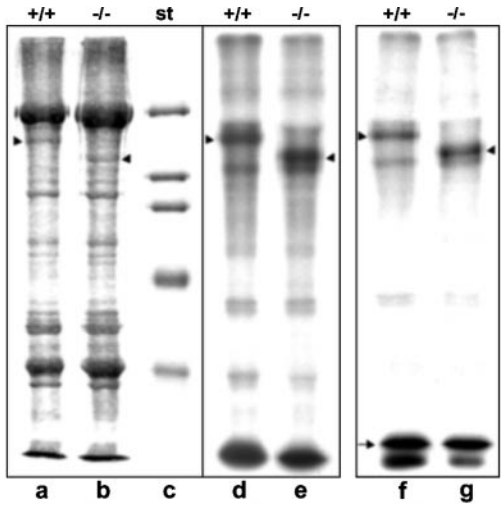

FIG. 5. **SDS-polyacrylamide gels (*lanes a–c*) and ^{32}P autoradiography (*lanes d–g*) of wild-type (+/+) and homozygous mutant fibers (−/−) from the left ventricle.** Samples were incubated with the catalytic subunit of cAMK in the presence of [γ-^{32}P]ATP. *st*, standard. *Arrowheads* point to the position of cMyBP-C. *Lanes d–e* correspond to the Coomassie Blue gels shown in *lanes a–b*. *Lanes f–g* are from a different experiment to demonstrate that major phosphorylation is associated, besides with cMyBP-C, with troponin I (*arrow*). Phosphorylation of TnI is known to cause a distinct decrease in Ca^{2+} sensitivity of force.

[γ-^{32}P]ATP revealed that both wild-type and the homozygous mutant cMyBP-C are phosphorylated to a similar degree (*arrowheads* in *lanes d–g*). Thus, the knock-in did not affect the phosphorylation of cMyBP-C, suggesting that the β-adrenergic pathway for this protein based on phosphorylation/dephosphorylation of the MyBP-C motif may still be intact.

DISCUSSION

The structural role of MyBP-C in both skeletal and cardiac myofibrils is well established (1–7); the C terminus of the protein, providing binding sites for myosin and titin, is essential for the formation and regular structure of thick filaments. Accordingly, C-terminal truncations of cardiac MyBP-C result in severe changes in heart ultrastructure and impaired cardiac mechanical performance, both in transgenic mouse models (18–20) and in FHC-affected humans (14, 16). It is perhaps not surprising that, of the about 30 mutations in the gene for cMyBP-C (*MYBPC3*) so far described in families with FHC, the majority locates to C-terminal domains (14). On the other hand, some mutations also occur in N-terminal regions of the molecule, but in these cases the mechanisms leading to FHC are more difficult to understand. A possibility is that N-terminal domains of cMyBP-C contribute to the regulation of cardiac-muscle contraction.

The knock-in mouse model presented here was generated in an attempt to uncover a possible (patho)physiological function of some of the N-terminal cMyBP-C domains. The knock-in was made bearing in mind that the cardiac isoform of MyBP-C is distinguished from the skeletal isoforms by two main features: (i) cMyBP-C contains an additional Ig domain, the C0 module (4, 5) and (ii) the MyBP-C motif between the Ig domains C1 and C2 can be phosphorylated by cAMP-dependent protein kinase and a calmodulin-dependent protein kinase (8, 28, 30, 31). The (reversible) phosphorylation mediates binding of the MyBP-C motif to the neck region of myosin (9, 10) and could be important for the hypothesized regulatory role of cardiac MyBP-C (11). Whereas the knock-in described here left the MyBP-C motif intact, it eliminated the N-terminal C1 domain and the linker sequence between C0 and C1 (Fig. 1). Thus, the mutant mice contain a shorter than normal cMyBP-C molecule whose size and domain architecture resemble those of the skeletal isoforms.

We bred the mice bearing mutant MyBP-C alleles to homozygosity, because we expected a relatively mild effect on cardiac structure and/or function; MyBP-C is not found in the entire A-band but forms 7–9 stripes in the A-band C-zone on either side of the M-line (32, 33). Indeed, hearts from both heterozygous and homozygous mutant mice showed no statistically significant changes at the ultrastructural level, and no differences were found between wild-type and heterozygous animals in terms of the force response of skinned cardiac fibers to Ca^{2+}-dependent activation. In contrast, fibers from homozygous mutant mice showed an increased Ca^{2+} sensitivity of force production (Fig. 4) whereas maximum force levels remained unchanged. This finding is consistent with that of an earlier study reporting that active tension at submaximal Ca^{2+} concentrations was increased, but maximum tension was not affected, upon partial extraction of MyBP-C from rat skinned cardiomyocytes (34). We note that extraction of MyBP-C was shown to slightly increase Ca^{2+} sensitivity at low to intermediate Ca^{2+} concentrations also in rabbit psoas muscle fibers, but the effect was much smaller than in cardiac cells (34). Our results extend the previous findings, suggesting that at least part of the change in Ca^{2+} sensitivity of cardiac sarcomeres may be related to a functional role of the N-terminal cMyBP-C domains.

One family of FHC patients has been described bearing a missense mutation (E258K) in the region just N-terminal to the MyBP-C motif (16). It is not unlikely that an altered function of N-terminal MyBP-C domains is responsible for the hypertrophy phenotype found in some members of this family. However, also clinically healthy individuals can carry the mutant *MYBPC3* allele (5, 16). Moreover, mutations in *MYBPC3* are frequently characterized by a mild phenotype particularly in young patients and a delayed age at the onset of symptoms (16, 17). Then, because the physiological background of human and mouse is very different, it is possible that the life span of the knock-in mice of this study is not long enough for significant

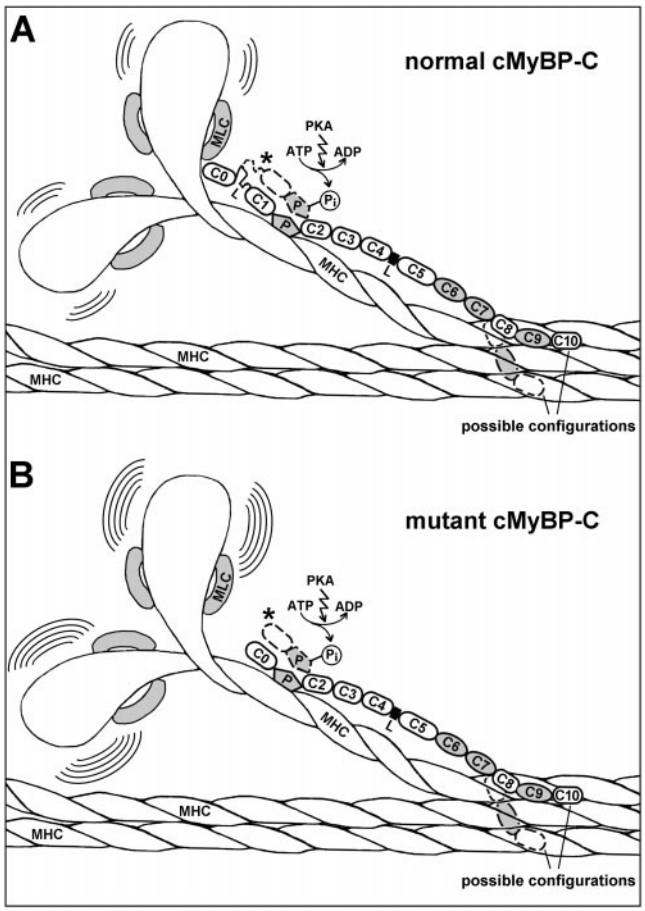

FIG. 6. **Schematic of proposed cMyBP-C influence on myosin-head mobility.** *A,* the wild-type cMyBP-C interacts with both the rod portion and the neck region of the myosin molecule. Phosphorylation of the MyBP-C motif by cAMP-dependent protein kinase (*PKA*) releases cMyBP-C from the myosin neck (*asterisk*). Interaction of the cardiac-specific C0 domain of MyBP-C with the myosin head would constrain cross-bridge movement. *B,* with the C1 domain plus adjacent linker missing, the N-terminal deletion mutant of cMyBP-C lacks the interaction with the myosin head, thereby decreasing steric hindrance of cross-bridge action permanently. Note that the length of the mutant cMyBP-C is comparable with that of skeletal MyBP-C isoforms. *MLC*, myosin light chain; *MHC*, myosin heavy chain; *C0–C10*, cMyBP-C domain numbers; *P*, MyBP-C motif; *L*, linker region.

changes of cardiac ultrastructure (and contractile properties of heterozygous animals) to occur. On the other hand, we demonstrated that the mutant protein is expressed and incorporated into the sarcomeres, which was associated in homozygous mutant animals with enhanced contractile performance. Taken together, N-terminal cMyBP-C mutations, if occurring in human heterozygous FHC patients, might in some instances determine a "hypercontractile" state that could induce cardiac hypertrophy directly. In this context we point out that a hypercontractile hypothesis has been put forth for some FHC cases in which other sarcomeric proteins are mutated, such as α-tropomyosin (35, 36). FHC might therefore be a disease induced by mutations causing either functional cardiac impairment followed by compensatory hypertrophy (apparently the majority of all cases) or functional enhancement followed by direct cardiac hypertrophy (14).

What mechanism(s) could be envisioned to explain the observed functional effect of the N-terminal deletion in cMyBP-C? Although the exact layout of MyBP-C in the thick filament is still subject to debate, structural details known to date (3, 10, 37) led us to propose a plausible model demonstrating the regulatory input by the protein. As shown in Fig. 6, cMyBP-C binds to the myosin rod (and titin) at the C terminus and also to the myosin neck region with the MyBP-C motif (in the unphosphorylated state). In the wild-type protein (Fig. 6*A*), the C0 domain at the N terminus could well interfere with the myosin head region, either by proximity to the regulatory light chains as proposed (10) or through specific interaction with the head. Indeed, a recent study suggested that the C0 domain of human cMyBP-C contains a novel putative myosin-binding site (38). Thus, in cardiac sarcomeres, MyBP-C could mechanically constrain cross-bridge movement in a manner not found in skeletal muscle. Phosphorylation-induced unbinding of the MyBP-C motif from the myosin neck region (Fig. 6*A*, *asterisk*) would release some constraints from the myosin head, thereby providing cardiac cells with an additional mechanism to regulate force development. In the case of N-terminal shortened cMyBP-C (Fig. 6*B*), the molecule may not be able to reach the myosin head region, which would change the flexibility or mobility of the cross-bridge permanently. Even though the number of myosin heads whose mobility can be affected by cMyBP-C is limited (because many heads lie outside of the C-zone), mechanical coupling of cross-bridges within a thick filament (12) would still produce an effect on contractile properties. A modulation of cross-bridge cycling rate may then alter the force response to Ca^{2+}-dependent activation. To summarize, a permanent increase in cross-bridge mobility caused by a shortened cMyBP-C would translate into higher force production and explain the observed mechanical changes.

An alternative model of cMyBP-C arrangement (not shown here) suggests that three molecules oriented perpendicularly to the fiber axis could overlap and form circular structures that tighten the packing of myosin filaments (3). Phosphorylation of the MyBP-C motif is thought to loosen the packing (39) by decreasing the overlap between the protein's N- and C terminus. The increase in circumference of the ring of cMyBP-C would facilitate regulated changes of actin-myosin interaction. Our results can be readily interpreted based on this "circular model." N-terminal deletion of an Ig domain plus adjacent linker sequence would most likely disrupt the protein ring, thus decreasing the restriction of myosin and improving actomyosin interaction. As in the above model, the actual length of MyBP-C would be important for the protein's regulatory impact. To conclude, molecular-level, mechanical effects of the knock-in generated here are explainable with available models of cMyBP-C arrangement.

In summary, we have produced a mouse mutant of cMyBP-C with N-terminal deletion whose characterization provided novel insights into the function of the protein. Knock-in mice stably expressed the deletion variant in the sarcomere, and cardiac fibers from homozygous mutant animals exhibited an increased Ca^{2+} sensitivity of force production concomitant with no change in maximum active force levels. The enhanced contractile performance may be caused by decreased steric hindrance of cross-bridge action by the shortened cMyBP-C. We also propose that the presence of additional N-terminal domains in the normal cardiac isoform of MyBP-C, compared with the skeletal isoforms, may be important to effectively regulate cardiac-muscle contraction at the cross-bridge level. Extension of these findings to humans suggest a molecular mechanism by which N-terminal mutations in cMyBP-C could cause familial hypertrophic cardiomyopathy.

Acknowledgments—We would like to thank Dr. Siegfried Labeit for continuous support and Sigrid Milan, Corinna Thiel, Ulla Gaio, and Monika Troschka for expert technical assistance.

REFERENCES

1. Offer, G., Moos, C., and Starr, R. (1973) *J. Mol. Biol.* **74,** 653–676
2. Yamamoto, K., and Moos, C. (1983) *J. Biol. Chem.* **258,** 8395–8401

3. Winegrad, S. (1999) *Circ. Res.* **84,** 1117–1126
4. Weber, F. E., Vaughan, K. T., Okagaki, T., Reinach, F. C., and Fischman, D. A. (1993) *Eur. J. Biochem.* **216,** 661–669
5. Carrier, L., Bonne, G., Bahrend, E., Yu, B., Richard, P., Niel, F., Hainque, B., Cruaud, C., Gary, F., Labeit, S., Bouhour, J. B., Dubourg, O., Desnos, M., Hagege, A. A., Trent, R. J., Komajda, M., Fiszman, M., and Schwartz, K. (1997) *Circ. Res.* **80,** 427–434
6. Alyonycheva, T. N., Mikawa, T., Reinach, F. C., and Fischman, D. A. (1997) *J. Biol. Chem.* **272,** 20866–20872
7. Freiburg, A., and Gautel, M. (1996) *Eur. J. Biochem.* **235,** 317–323
8. Gautel, M., Zuffardi, O., Freiburg, A., and Labeit, S. (1995) *EMBO J.* **14,** 1952–1960
9. Gruen, M., and Gautel, M. (1999) *J. Mol. Biol.* **286,** 933–949
10. Gruen, M., Prinz, H., and Gautel, M. (1999) *FEBS Lett.* **453,** 254–259
11. Kunst, G., Kress, K. R., Gruen, M., Uttenweiler, D., Gautel, M., and Fink, R. H. A. (2000) *Circ. Res.* **86,** 51–58
12. Winegrad, S. (2000) *Circ. Res.* **86,** 6–7
13. Watkins, H., Conner, D., Thierfelder, L., Jarcho, J. A., MacRae, C., McKenna, W. J., Maron, B. J., Seidman, J. G., and Seidman, C. E. (1995) *Nat. Genet.* **11,** 434–437
14. Bonne, G., Carrier, L., Richard, P., Hainque, B., and Schwartz, K. (1998) *Circ. Res.* **83,** 580–593
15. Mogensen, J., Klausen, I. C., Pedersen, A. K., Egeblad, H., Bross, P., Kruse, T. A., Gregersen, N., Hansen, P. S., Baandrup, U., and Borglum, A. D. (1999) *J. Clin. Invest.* **103,** R39–43
16. Niimura, H., Bachinski, L. L., Sangwatanaroj, S., Watkins, H., Chudley, A. E., McKenna, W., Kristinsson, A., Roberts, R., Sole, M., Maron, B. J., Seidman, J. G., and Seidman, C. E. (1998) *N. Engl. J. Med.* **338,** 1248–1257
17. Charron, P., Dubourg, O., Desnos, M., Bennaceur, M., Carrier, L., Camproux, A. C., Isnard, R., Hagege, A., Langlard, J. M., Bonne, G., Richard, P., Hainque, B., Bouhour, J. B., Schwartz, K., and Komajda, M. (1998) *Circulation* **97,** 2230–2236
18. Yang, Q., Sanbe, A., Osinska, H., Hewett, T. E., Klevitsky, R., and Robbins, J. (1998) *J. Clin. Invest.* **102,** 1292–1300
19. Yang, Q., Sanbe, A., Osinska, H., Hewett, T. E., Klevitsky, R, and Robbins, J. (1999) *Circ. Res.* **85,** 841–847
20. McConnell, B. K., Jones, K. A., Fatkin, D., Arroyo, L. H., Lee, R. T., Aristizabal, O., Turnbull, D. H., Georgakopoulos, D., Kass, D., Bond, M., Niimura, H., Schoen, F. J., Conner, D., Fischman, D. A., Seidman, C. E., and Seidman, J. G. (1999) *J. Clin. Invest.* **104,** 1235–1244
21. Schmidt, C., Bladt, F., Goedecke, S., Brinkmann, V., Zschiesche, W., Sharpe, M., Gherardi, E., and Birchmeier, C. (1995) *Nature* **373,** 699–702
22. Ramirez-Solis, R., Rivera-Perez, J., Wallace, J. D., Wims, M., Zheng, H., and Bradley, A. (1992) *Anal. Biochem.* **201,** 331–335
23. Krämer, J., Aguirre-Arteta, A. M., Thiel, C., Gross, M., Dietz, R., Cardoso, M. C., and Leonhardt, H. (1999) *J. Mol. Med.* **77,** 294–298
24. McKenna, W. J., Stewart, J. T., Nihoyannopoulos, P., McGinty, F., and Davies, M. J. (1990) *Br. Heart J.* **63,** 287–290
25. Linke, W. A., Rudy, D. E., Centner, T., Gautel, M., Witt, C., Labeit, S., and Gregorio, C. C. (1999) *J. Cell Biol.* **146,** 631–644
26. Dohet, C., Al-Hillawi, E., Trayer, I. P., and Rüegg, J. C. (1995) *FEBS Lett.* **377,** 131–134
27. Herzig, J. W., Köhler, G., Pfitzer, G., Rüegg, J. C., and Wölffle, G. (1981) *Pflügers Arch.* **391,** 208–212
28. Venema, R. C., and Kuo, J. F. (1993) *J. Biol. Chem.* **268,** 2705–2711
29. Hofmann, P. A., and Lange, J. H. (1994) *Circ. Res.* **74,** 718–726
30. Hartzell, H. C., and Glass, D. B. (1984) *J. Biol. Chem.* **259,** 15587–15596
31. Schlender, K. K., and Bean, L. J. (1991) *J. Biol. Chem.* **266,** 2811–2817
32. Dennis, J. E., Shimizu, T., Reinach, F. C., and Fischman, D. A. (1984) *J. Cell Biol.* **98,** 1514–1522
33. Bennett, P., Craig, R., Starr, R., and Offer, G. (1986) *J. Muscle Res. Cell Motil.* **7,** 550–567
34. Hofmann, P. A., Hartzell, H. C., and Moss, R. L. (1991) *J. Gen. Physiol.* **97,** 1141–1163
35. Bottinelli, R., Coviello, D. A., Redwood, C. S., Pellegrino, M. A., Maron, B. J., Spirito, P., Watkins, H., and Reggiano, C. (1998) *Circ. Res.* **82,** 106–115
36. Bing, W., Redwood, C. S., Purcell, I. F., Esposito, G., Watkins, H., and Marston, S. B. (1997) *Biochem. Biophys. Res. Commun.* **236,** 760–764
37. Gilbert, R., Cohen, J. A., Pardo, S., Basu, A., and Fischman, D. A. (1999) *J. Cell Sci.* **112,** 69–79
38. Flavigny, J., Souchet, M., Sebillon, P., Berrebi-Bertrand, I., Hainque, B., Mallet, A., Bril, A., Schwartz, K., and Carrier, L. (1999) *J. Mol. Biol.* **294,** 443–456
39. Weisberg, A., and Winegrad, S. (1996) *Proc. Natl. Acad. Sci. U. S. A.* **93,** 8999–9003